Biomaterials Connect

ISSN: 3105-0387

2025, Vol. 2, Cite as: doi:10.x/journal.x.x.x

SCIFINITI PUBLISHING

OPEN ACCESS

Research Article

COMPUTATIONAL SIMULATIONS-OPTIMIZATION OF UHMWPE KNEE ARTHROPLASTY LINEAR ABRASIVE WEAR

Francisco Casesnoves[1]

Independent Researcher, Tallinn, Harjumaa, 12618, Estonia

casesnoves.research.emailbox@gmail.com

ABSTRACT

Today, total knee artificial implants constitute (TKA) a high-demanding prostheses in biomechanical/surgical-orthopedics industry. Abrasive TKA linear wear model-algorithm computational simulations are developed and presented for ultra-high molecular weight polyethylene (UHMWPE). This material is widely used for TKA implants. The implemented mathematical model is the classical/modified Archard's model modified for TKA linear abrasion. The algorithms for Integer and Integral Formulation are explained. For computational intelligence simulations, selected literature experimental data, both *in vitro* and *in vivo*, is set within programming software. 3D Imaging-processing computational simulations software in 3D are designed with Graphical Optimization and Interior Optimization techniques. Million Cycles (Mc) results for Linear Wear, in numerical dataset and 3D simulations image-processing graphs are demonstrated and compared to literature database. Useful Biotribology/Biomaterials and Biomedical TKA clinical/manufacturing applications are briefed.

Keywords: total knee artificial implants; 3D simulations; graphical optimization; linear wear; mathematical model; 3D Imaging-processing; ultra-high molecular weight polyethylene.

1. INTRODUCTION AND OBJECTIVES

The biomechanics and TKA are rather complicated by several factors. First, its most important function is the total weight support as the third biomechanical system of the anatomy, [1,2], (first system in head-neck, second is thorax-abdomen-spine-hip, and third is knee-feet). That is, the legs and the feet. The second reason is the biodynamics of walking and movement, which require balance and support for the body's center of gravity. The third, and not the less, is that the articulations of knee, ankle, and feet constitute an essential biomechanical system for walk and basic life movements. Complementary reasons are the biomedical cartilage and bone aging-degeneration and forced movements injuries probabilities. All of them are mutually synergic and constitute an interrelated biomechanical system [1-4]. In other words, if the knee joint cartilage degenerates soon, causes a bone damage, this creates instability and balance loss at knee, and in consequence the movement dynamics is limited or impeded. Just remind that histologically cartilage cells cannot regenerate like the elastic skin fibers (up to current

science-research, it is tried to resolve the problem with stem cells, but that matter is out of this research scope). That is, any individual is born to get a fixed number of skin-organs elastic fibers and cartilage cells when his growth-development is completed. The menisci function, which resembles in a biomechanical dumping-sense the intervertebral disks, proves the natural design to cope with so high biodynamical loads/enforced-movements. Furthermore, the second biomechanical system, in particular the hip articulation, can be damaged by forced/biased movements and biomechanical abnormal load distributions at knee joint. All this briefing gives a basic idea of the complications that may occur in surgical pathology and biomechanical diseases at knee articulation.

On the other hand, and also, knee injuries, joint traumatological pathologies, and concomitant rheumatological or infection diseases, creates a high medical-industrial demand. Then, the economic cost, [1-8], is rather high for both public, private, or mixed health services at many countries. Therefore, TKA investigation for reliability and high-durability of new TKA prostheses is among the current priorities in biomedical industry. Biomathematical studies with optimization modelling take the task for wear prediction and durability of TKA prostheses. An additional question is the number of model variants and large amount of different testing laboratories. This implies the requirement for standards methods both experimental and theoretical-modelling. In this contribution, the most usual standards, ISO-related, [1-11], are prioritized for the objectives of the study. For femoral component, Figure 1, Cobalt-chrome is mostly used, with several variants [3,11].

Previous contributions address usually Finite Elements studies in 2D; however, this study focuses mainly in 3D Graphical Optimization. Those are made exclusively in FE [3,11], or with/without in-vitro/in-vivo cadaveric comparisons [12-18]. Since studies in vivo present the linear wear data usually in mm/year or mg/year (this in general for Volume Wear), and the in vitro research is expressed in mm/Mc, it is necessary to approximate the average Mc that a standard patient performs in a year, [16]. Here it was set for calculations approximately 2Mc per year, [16]. The specification of Archard's laws (fundamental, differential, and modified), and standard units, are not expressed for most researchers with detailed explanations/variants [12-18]. Also, the utility of presented algorithms for implementation in FE or simple simulations should be detailed for other researchers options be set clearly/fastly. This article shows solutions for these hurdles in the simplest form. Additionally, the 3D innovative Graphical Optimization charts that are shown/developed constitute a complement related to other literature graphics.

The mathematical equations and models used are for Linear Abrasive Wear (in mm) without Creep and Lubrication Factors [3] at this stage. For Volume Wear (in mm^3), the Finite Elements Method is widely applied [1-11]. Compared to Finite Elements method, this direct algorithm implementation in 2D-3D graphical optimization offers some advantages. The first one is that it is less laborious and requires less time than Finite Elements. The second is that to implement several algorithms at the same time within one single program is easy and gives comparisons. In brief, fast-adaptation of the programming algorithm offers an objective advantage related to FE method, both as laboratory tool and as tentative initial approximation. What is more, this algorithmic technique is useful to be implemented with FE method or get a database for further application of FE method.

Therefore, the computational model gets innovations/advances from previous ones for a number of reasons. First, it comprises all published range of the linear wear constant, K_w, [3], namely [2.20×10^{-7}, 10^{-6}] approximately. At several figures values range of Kw are multiplied by 10^{-3} because of the software-settings units for 3D images. Second, it plots in 2D-3D all the standard loads range, combined with the computational calculations (vectors) for K_w range. Third, the Million Cycles (Mc) range is set computationally at 2D-3D multiple-graphics in pattern with those loads and K_w ranges, Figure 2. Another advantage is the usage of 3D surfaces to guess/search for optimal settings-up when preparing to use FE method.

In summary, after these fundamental concepts introduction, the study is focused on biomechanical models' computational intelligence-optimization and practical numerical and image processing results for mainly ultra-high molecular weight polyethylene (UHMWPE).

1.1 The Biomechanical Concepts of Knee Articulation

At Figure 1, it is shown the basic knee biomechanical system after TKA implantation (parts and movement concepts). For normal life, the knee articulation supports biomaterials stress, loads, flexions, extensions, torsions, rotations and more complicated movements. Furthermore, it is not exclusively the articulation, ligaments, e. g., cruciate ones, and external, internal, lateral ligaments form a rather complicated articulated biosystem. This makes the incidence/prevalence of knee biomechanical pathology rather frequent. The sport activity increases these risks of injuries, and in that field, the knee articulation supports loads and extreme movements continuously, [1,2,5,6,10]. The sport-medicine specialization for knee is a branch with deep knowledge and applications.

1.2 Biomechanical Knee Implants

TKA medical industry is profuse and offers a large number of alternatives. The most common TKA prostheses resemble the femur natural condyles, that is, they are bicompartmental. However, monocompartmental TKA prostheses have also been developed. For the standard TKA, the number of variants, related to biomaterials, biomechanical design, and forces-distribution designs are rather high. This makes complicated the laboratory testing analysis, both *in vitro* and *in vivo*. Further, the wear, creep, lubrication and other biomechanical parameters differ substantially in literature for the amount of methods, techniques, and laboratory apparatus, ISO variants are large also. All in all, the TKA study towards future constitutes a difficult biomechanical and biopathological field actually, [1,2,5,6,10,11].

Figure 1.- [Google free images, Dr. Albrecht, knee and cartilague specialist, website, https://www.knieschmerzen-wien.at/albrecht-christian-en.html], modified and drawn by Francisco Casesnoves. The sketch is completed with main parts of TKA. Inset, the most important anatomical parts are marked. Note that the femur condyles are made in steel, and the tibial plateau is polyethylene.

1.3 Objectives of Study

The objectives of the study are primary and secondary ones. The primary objective is to develop computational intelligence software efficacious and useful for accurate simulations. That is in order to presents practical data for TKA research. The second main objective is to demonstrate how 2D-3D simulations and optimization of TKA can be useful for the previous intention. Secondary, applications, algorithmic developments, and mathematical proofs are shown. At this stage, Creep and Lubrication Factors for the models were not set [3], (Algorithms 1 and 2).

In brief, the article presents Computational Intelligence simulations and 2D-3D Graphical Optimization for PE TKA abrasive. Results coincide in magnitude order with standard laboratory measurements and literature publications. New software for mathematical models was originally created and Biomechanical-Biotribology applications are briefed.

2 MATERIALS AND METHODS

Primary approximations are to consider exclusively the TKA wear, and exclude Creep and Lubrication Factors, (algorithms 1 and 2). Therefore, the calculations of this study constitute the linear wear optimization-determination to get wear durability predictions of the TKA implant with fundamental physical formulation [3,11]. In the literature, variations of models are applied, e.g. [19], however the most applied is Archard's model with several variants [3,11]. Basic measurements taken into account in this study for in vitro and in vivo and contact area correspond to [12-18]. Typical values of TKA wear, most times obtained by FE method are referred at [18-34]. It is not considered at present Archard's Volume Wear, e.g. [20], for this study.

2.1 The basic Model algorithm(s)

The basic algorithm-model from [3,11], applied and analyzed reads,

$$\textit{The Archard's Model applied on TKA,}$$

$$L_{wear} = K_{wear} \sum_{j=1}^{N} \left[\sum_{i=1}^{n} p_i \, |\overrightarrow{v_i}| \, \triangle t_i \right]_j ;$$

Algorithm (1)

where,

L_{wear} : Linear abrasive wear (mm).

K_{wear} : Wear constant, standard (mm^3 / N mm). Note: at figures values range of K_w are usually multiplied by 10^{-3}.

p_i : Pressure (N / mm^2).

v_i : Sliding discrete Velocity for discrete time increment (mm / s).

Δt_i : Discrete time interval (s).

i, j : Summatory indexes. The [**i**] is for velocity variation within a cycle (n). The [**j**] is for cycles number (N).

2.1.1 The Creep and Friction Factors

Creep

Although those factors are not applied in the study, description with details of the Creep and Lubrication formulas are conveniently shown. For Creep, [3], the model-equation format (Lee and Pienkowski, 1998) reads,

Algorithm (2)

$$The\ Archard's\ Model\ complemented\ with\ Creep,\ applied\ on\ TKA,$$

$$L_{total\ wear} = L_{linear\ wear} + L_{creep};$$

$$Hence,$$

$$L_{total\ wear} = L_{linear\ wear}\ [K_1 + K_2\ (log\, t\ - 4)]\ P_{average}\, h;$$

where,

K_1 : Model Constant, [3]. Values for K_1 and K_2 are respectively , 3.491×10^{-3} and 7.961×10^{-4} .

K_2 : Model Constant, [3]. Values for K_1 and K_2 are respectively , 3.491×10^{-3} and 7.961×10^{-4} .

t: Time of load (minutes) .

$P_{average}$: (N/mm^2)

h : Polyethylene thickness (mm)

Friction

One common Friction Factor, set within the general formula is: **$[1+3\ \mu^2]^{½}$**, [21-23], with values for UHWMPE of around [10^{-2}] magnitude order. This Friction factor multiplies linearly the general formula (1). At this stage, it is not applied in the study. Friction was not set at this stage because the friction value in this case is, approximately,

$(1+3 \times 0.072)^{0.5}$ = 1.0073, [a dimensional]

(2)

That is, a magnitude order of 10^{-3}. This implies that the magnitude difference if set within algorithms would not determine a magnitude order significance. That precision is useful for further refinements.

2.1.2 The Integral Algorithm

It is convenient, when experimental data or database available, to compute the algorithm in integral-equation of first kind. Hence, taking trivial limits for getting an integral form,

The Archard's Model applied on TKA, integral form,

$$L_{wear} = K_{wear} \sum_{j=1}^{N} \sum_{i=1}^{M} \left[\int_{0}^{t_i} p \, |\vec{v}| \, dt \right]_j ;$$

Algorithm (3)

where,

L_{wear} : Linear abrasive wear (mm) .

K_{wear} : Wear constant, for programs (mm^3 / N mm) . Note: at figures values range of K_w are usually multiplied by 10^{-3} because of this change of units (generally K_{wear} is formulated (mm^3 / N x m) .

p(t) : Instantaneous pressure (N / mm^2) . Function of time.

v(t) : Instantaneous sliding velocity for integral. Function of time (mm / s) .

dt : Differential of time during i-interval (s) .

i ; Summatory index for time at every integral for a cycle (M).

j ; Summatory index for total cycles (N) .

Proof

$$The\ Archard's\ Model\ applied\ on\ TKA,\ integral\ form\ proof,$$

$$For\ one\ cycle,$$

$$L_{w1} = K_w p S;$$

$$where\ S\ is\ sliding\ distance,\ hence$$

$$L_{w1} = K_w p\, v\, t;$$

$$therefore, provided\ \vec{v}\ constant\ and\ taking\ derivatives\ for\ time\ variable\ ,$$

$$\frac{dL_{w1}}{dt} = K_w p\, v\ ;\ or,$$

$$dL_{w1} = K_w p\, v\, dt,\ integrating,$$

$$\int_0^t dL_{w1} =$$

$$K_w \int_0^t p\, v\, dt,\ supposing\ instantaneous\ pressure\ and\ sliding\ velocity\ during\ one\ cycle\ ,$$

$$Therefore, taking\ N\ cycles,\ and\ integrating,$$

$$L_{wear} = K_{wear} \sum_{j=1}^{N} \sum_{i=1}^{M} \left[\int_0^{t_i} p\, |\overrightarrow{v}|\, dt \right]_j ;$$

[Casesnoves Bioengineering Laboratory Algorithm 3114]

2.2 Computational intelligence Dataset Software

Dataset selected from literature is set in wide ranges at programs, because the commercial materials, TKA sizes, and Algorithm constants applied differ among authors, laboratories, testing apparatus, testing temperature, etc. Therefore, the practical objective of the simulations-optimizations is to provide with large scale range that can be used to predict durability for all of those variants. Software is based on hip wear previous Author's contributions for hip wear programming design [35,36]. General additional biotribology database can be found at [37-39].

2.2.1 Benchmark polyethylene model

There are variations for the TKA size in literature about laboratory studies. However, the size used for simulation software implementation was the most standard one, [1]. That is, 78.2 x 44.2 mm the total coronal dimension, from that magnitude the contact surface was approximated-calculated. That size is according to ISO, and it is noteworthy to consider that there are ISO variants.

2.2.2 Sliding Distance (SD)

Sliding distance recommended by ISO is about 80 mm [10]. However, it was set 60 mm, taking into account differences between prostheses sizes, [12].

2.2.3 Load

This is a magnitude convergence point for most of studies. The most usual assumed magnitude by majority of investigations [21-23]. For example [2] (page 63), Table 1 & 2 gives an overview of the changes of loads and gaits from normal walk to down stairs/ramp. Figures 1-8 show extensive imaging-processing data. From this Table and setting a patient average weight of 75 kg, the interval of loads that comprise approximately walk, stairs and climb down/up, etc, can be deducted. Usually, then, is [2000, 2600] N interval. Here it is taken a maximum of 2300-2600 N in most simulation-programs. Other Authors, [21], apply a maximum load of 3000 N. That is not considered for this study.

2.2.4 Standard Unit System

The Linear Wear standard TKA erosion Archard's model units used in literature, most times, are mm^3 of eroded material or mm depth of erosion along contact surface. When studies are in vivo or provided with cadaveric history, the Linear Wear is given in mm/year. It is not an objective of this study to discuss the optimal unit system. Instead, the image-processing and numerical data is expressed in mm depth to bring for user the choice to compare dataset appropriately, [3,11]. The numerical comparative approximations constitute an important part of this study for numerical dataset in mm/year. This is done taking into account the average Mc for a year, [16], which is about 2Mc/year. The physics dimension equations for Linear and Volume Abrasive Wear are explained in (3).

2.2.5 Standard Abrasive Wear K_w Magnitude

Given the fact that the number of laboratory apparatus, measuring systems, and hybrid studies are profuse, in the literature, there is not a total agreement for K_w magnitude [3]. Introduction, Figure 1 shows 2D GNU-Octave imaging processing polynomial fit that describes the variation in function of K_w variation and Million Cycles [13-23] integer interval. Note: at figures values range of K_w are usually multiplied by 10^{-3}.

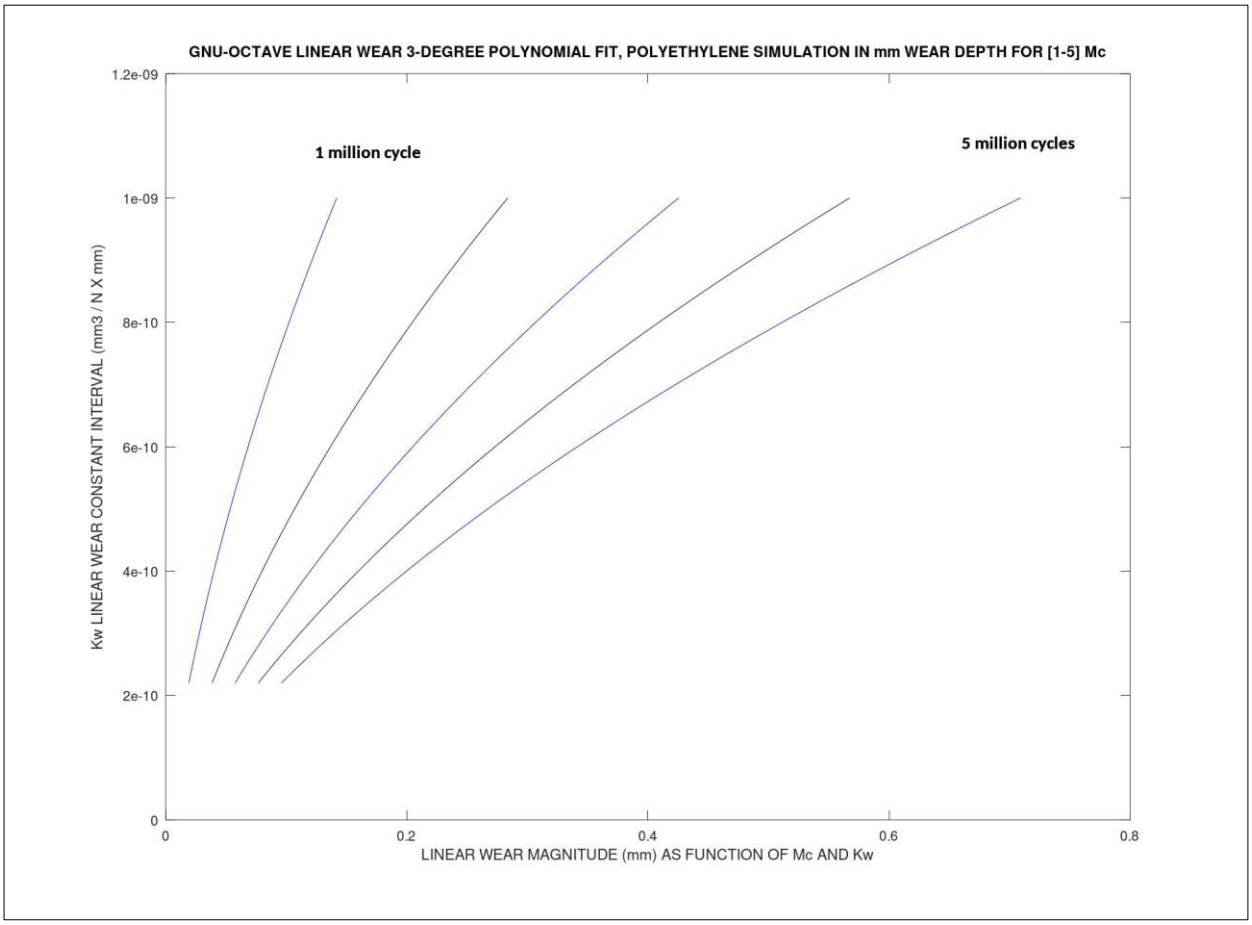

Figure 2.-For parameters of Tables 1-2, example of polynomial fit for wear prediction in function of the variation range of [K_w x 10^{-3}], (continuous), and Mc [1,5] (integer). It is clear the magnitude variation related to increase of [K_w x 10^{-3}], and the Mc number. Note: at figures values range of K_w are usually multiplied by 10^{-3} . Previously the 2D imaging processing,a 3-degree polynomial fit was developed for every million-cycle graph-line type. This type of software is developed from Author's series of previous publications in hip prostheses wear and other computational contributions.

Standard literature units for Archard's model dimension equations, For example,

Erosion in mm depth,

$$L_w\,(mm\,depth) = K_w\,(\tfrac{mm^3}{N\,mm})\,Pressure\,(\tfrac{N}{mm^2})\,Sliding\,Distance\,(mm);$$
$$as\,a\,result\,, L_w\,is\,in\,mm,$$

Erosion in mm^3 eroded material volume,

$$V_w\,(mm^3 volume) = K_w(\tfrac{mm^3}{N\,mm})\,PressureForce(\,N\,)Sliding\,Distance(mm);$$
$$as\,a\,result\,, V_w\,is\,in\,mm^3;$$

(3)

The first one is the primary method applied in this paper. That is Abrasive Linear Wear.

Table 1.- Selected Dataset used for simulations and optimization software. Disclaimer: some variants were applied for trial programs and images. Note: at figures many times values axe-range of K_w are multiplied by 10^{-3}. Figures 1-8 show extensive imaging-processing data.

SELECTED DATASET USED FOR SIMULATIONS			
PARAMETER AND UNITS	**INTERVAL OR MAGNITUDE SOFTWARE IMPLEMENTED**	**REFERENCES**	**COMMENTS**
LOAD (N)	[2000,2300-2600]	[1,11,21-23]	Standard magnitude, usually agreed by most authors.
SLIDING DISTANCE (mm)	60	[10]	ISO Standard, it varies according to studies.
K_W (mm^3 / (N x mm)	[2.20 x 10^{-7}, 10^{-6}] [Note: at figures values range of K_w are usually multiplied by 10^{-3} because all the units are set in mm at software]	[3,21-23]	The constant K_W has different values in literature. It is implemented an interval that comprises most published magnitudes.
LOAD SURFACE (mm^2)	[1000 , 2300-2600]	[21-23]	This varies significantly according to several publications.
CYCLES NUMBER	[1, 5]	[1-11, 13-34]	It is presented, usually, in most books and

(in M (millions)) **notation standard: Mc**	image-processing is shown for [1, 5] Mc	[1-10]	papers dataset from 1 M to 5 M. Most authors show predictions and calculation testing for 1-5 Mc.
IMPLEMENTED: **K_W (mm^3 / (N x mm)) x 10^{-3}** **according to (3)**	[2.20 x 10^{-10}, 10^{-9}]	[3]	K_W has different magnitude according to authors, [3], and some researchers propose values of K_W , for example [21-23] .
Poisson ratio and Elastic modulus, Density, for UHMWPE	**NOT IMPLEMENTED,** **EXCLUSIVELY ILLUSTRATIVE** **UHWMPE: Young's modulus 463 MPa, Poisson' ratio 0.46, density 960 kg/m^3 [21-23].**	[21-23]	N/A for the algorithms which are programmed.

Table 2.- Selected Dataset literature and Author sources for Table 1. It is very frequent to find different magnitude orders for K_W in the literature. The current name for this constant is wear coefficient. Recently for new models it was applied an adimensional constant called wear factor.

DATASET REFERENCE SOURCES DISSCUSED		
PARAMETER AND UNITS CRITERIA	**LINEAR-WEAR DETAILS AND REFERENCES FOR SOFTWARE IMPLEMENTED**	**JUSTIFICATION**
LOAD (N)	[1,11,21-23] Loads depend in many times on ISO experimental system used. Therefore. Magnitudes are not standard. The most interval applied in the literature is [2000,2300-2600] . However, some Author's, [21], apply loads of 3000 N, which is considered too high. In the same way, [10], magnitude of 1200 N is too low.	Standard magnitude, usually agreed by most authors.
SLIDING DISTANCE (mm)	[10] Sliding distance varies along the literature. It was selected the most frequent magnitude. Besides, the dataset choice comprised exclusively those referred to ISO standards. Interval, [10], is approximated [38.7, 83.7] mm.	ISO Standard, it varies. It is necessary to select the most frequent interval.
K_W (mm^3 / (N x mm)	[3, 21-23] It is very frequent to find different magnitude orders for K_W in the literature. The current name for this constant is wear coefficient. Recently for new models it is applied an adimensional constant called wear factor.	The, [3], range is applied for software.

LOAD SURFACE **(mm^2)**	[21-23] The magnitude value intervals comprise the most frequent along the literature.	**[**1] shows standard coronal size and loads.
CYCLES NUMBER **(in M (millions))** **notation standard: Mc**	[1-11, 13-34] In the literature, the results, when using Mc, are shown for 1 to 5 usually. Ms is the most standard form to present the linear and volumetric wear.	It is presented, usually, dataset from 1 Mc to 5 Mc . In Figure 7 it is shown one 1-6 Mc composition with numerical results.
IMPLEMENTED: **K_W (mm^3 / (N x mm)) x 10^{-3}** **according to [3]**	[3] Both wear coefficient and the recent for new models wear factor show differences along literature. In [3], large data shows a variation in one magnitude order.	Table 1 interval, is considered sufficient confident interval that comprises almost all authors publications.

2.3 Computational intelligence Software

We developed software programming mainly from previous experience in hip wear models [35,36]. Systems used were Matlab® 2023 and GNU-Octave® 7.1.0. For programming algorithms 1-2, the difficulty was the matrices congruency and the loops for arrays.

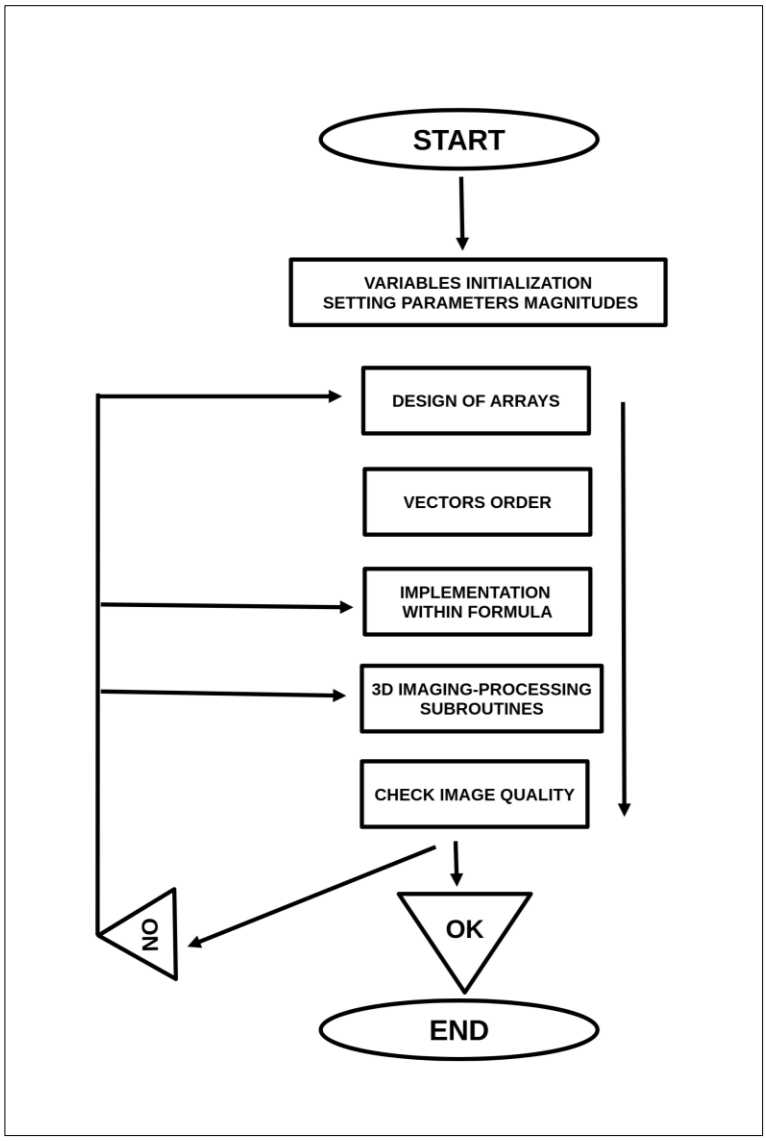

Figure 3.-Basic programming flow chart. The most important of those programs are the arrays and their implementation within the algorithm. If the dataset-vectors are not conveniently re-arranged and set at the 3D imaging processing subroutines, the resulting image could not be acceptable. Note: at figures many times values axe-range of K_w are multiplied by 10^{-3}. This type of software is developed from Author's series of previous publications in hip prostheses wear and other computational contributions [35, 36, 40, 41, 42, 43, 44, 45-51, 52, 53-63].

3 RESULTS AND DISCUSSION

Results are divided into Graphical and Numerical. In this primary stage, the numerical ones were determined by Matlab graphical methods. The sharpness of 3D Graphical optimization is acceptable, and numerical figures show approximate coincidence with standard literature [13-18], Numerical results are shown in Table 3, and comparisons at Table 4.

3.1 3D Graphical Optimization Results

We developed Linear Wear Graphical Optimization Method based on previous publication series of Volume Wear hip arthroplasty, [35,36]. It essentially consists in finding the global/local minima by using the 3D imaging surfaces of the algorithm objective function plus two selected parameters. Here it is applied on the wear formulas (1,2) to determine the optimal minima or any desired values subject to particular constraints along the 3D surface. In Ilustrative Example 1, it can be seen the process initiation. Firstly some tentative programs are designed, after that, when checking the functionality of the software and the numerical congruence of the 3D graphs, the definite 3D Graphical Optimization Image-Processing charts are done with accurate parameters and interval. Note: at figures many times values axe-range of K_w are multiplied by 10^{-3} because of units. Figures 4-9 show all the Graphical Optimization results with dataset. Figures 10-13 show extensive imaging-processing of results. The main references that are suggested for the reader to get knowledge about computational intelligence software are useful, [35, 36, 40, 41, 42, 43, 44, 45-51, 52, 53-63]. In those references the reader can find precise programming charts. The references [56-61] are intended for complementary further reading in polymer materials, biomechanics and tribology, recommended for the reader.

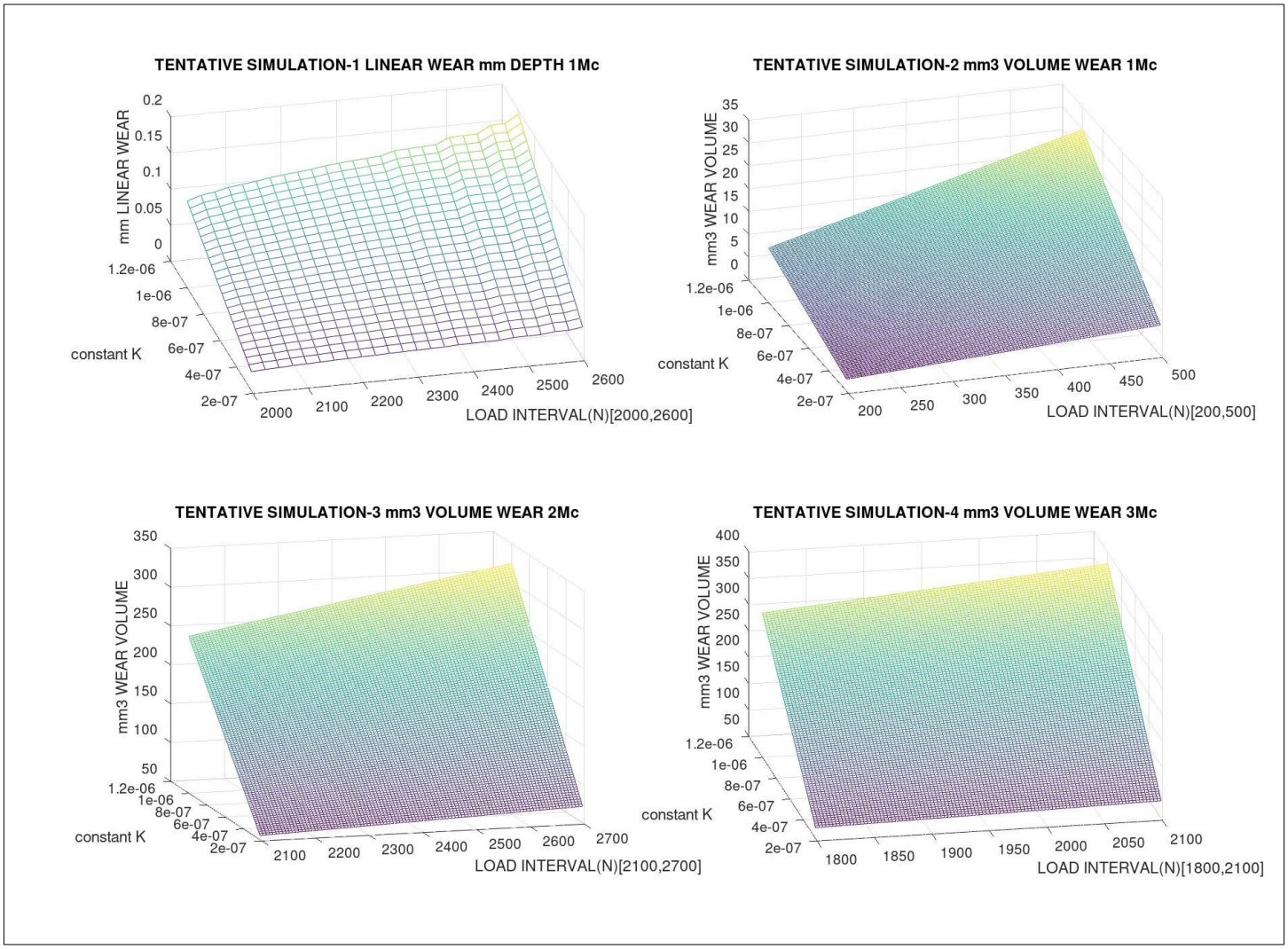

Figure 4 .- First trial tentative quadruple-simulation with GNU-Octave and two different 3D imaging processing subroutines. The intention is to check the different image qualities and the correct running of the programs. It is shown the basic model simulated in wear mm depth (when the surface contact is

implemented), image 1, and the basic model simulated in wear mm^3 volume, images 1-4. Since it is tentative to show the computational method, magnitude-parameters model are not too much exact. Matlab programs are equivalent. [Casesnoves Bioengineering Laboratory Software 2025-k-1]. The loads are varied intervals, the K constant interval is approximately [10^{-6} , 10^{-7}] . Note: at figures, not precisely here, many times values axe-range of K_w are multiplied by 10^{-3} .

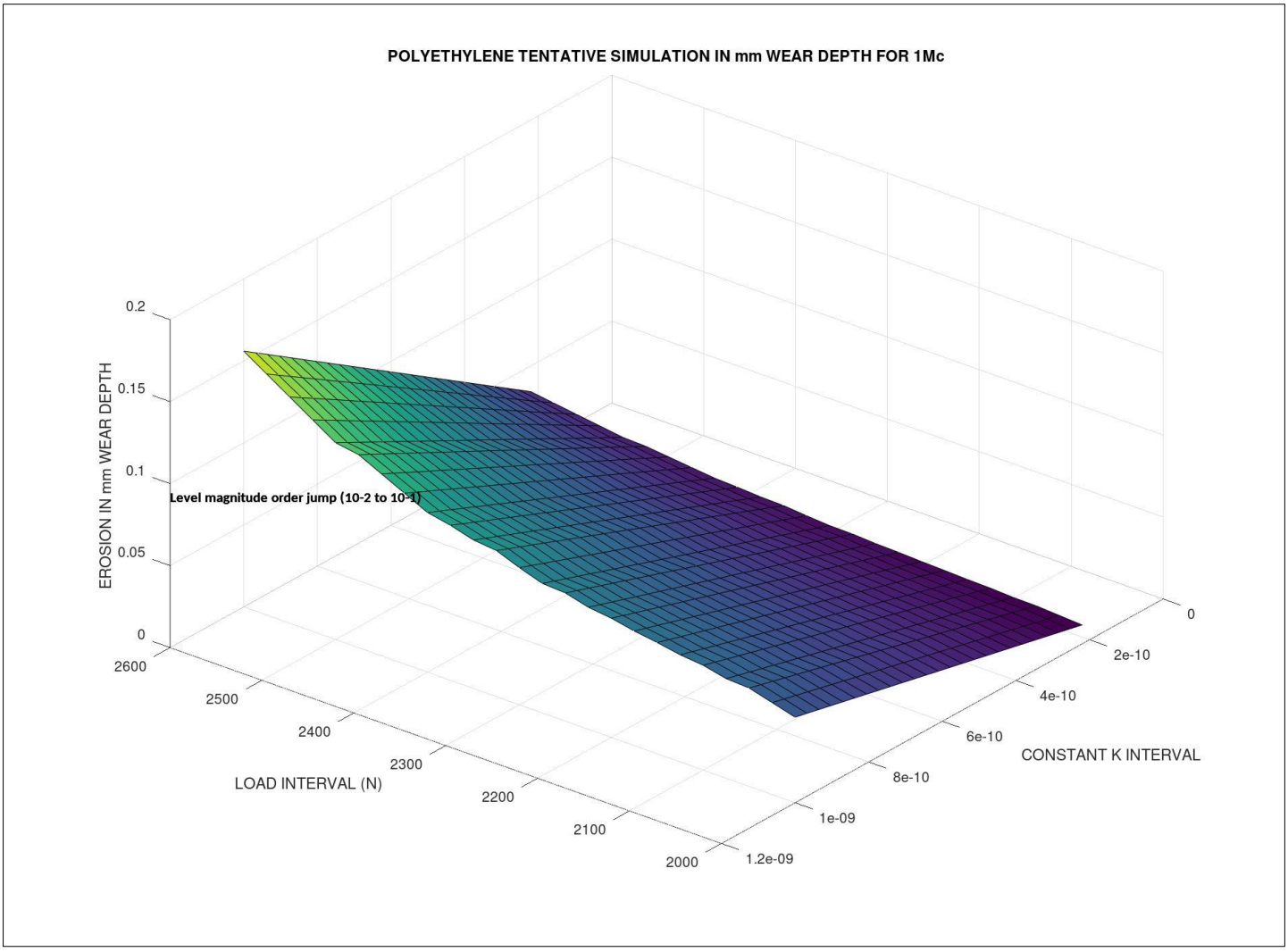

Figure 5.- Continuing the software improvements, second trial tentative simulation with GNU-Octave. It is shown the basic model simulated in wear mm Linear Depth (when the surface contact is implemented, [1-8]). At tentative, it was clear the magnitude order jump around 2300 N load from 10^{-2} to 10^{-1}. It is set 1 Mc. Since it is tentative to show the computational method, magnitude-parameters model are not too definite, but approach experimental laboratory literature, [1-8], Matlab programs are equivalent, and in general Matlab 2D-3D image quality is superior than GNU-Octave, [Casesnoves Bioengineering Laboratory Software 2025-k-2]. Note: at figures many times values axe-range of K_w are multiplied by 10^{-3}.

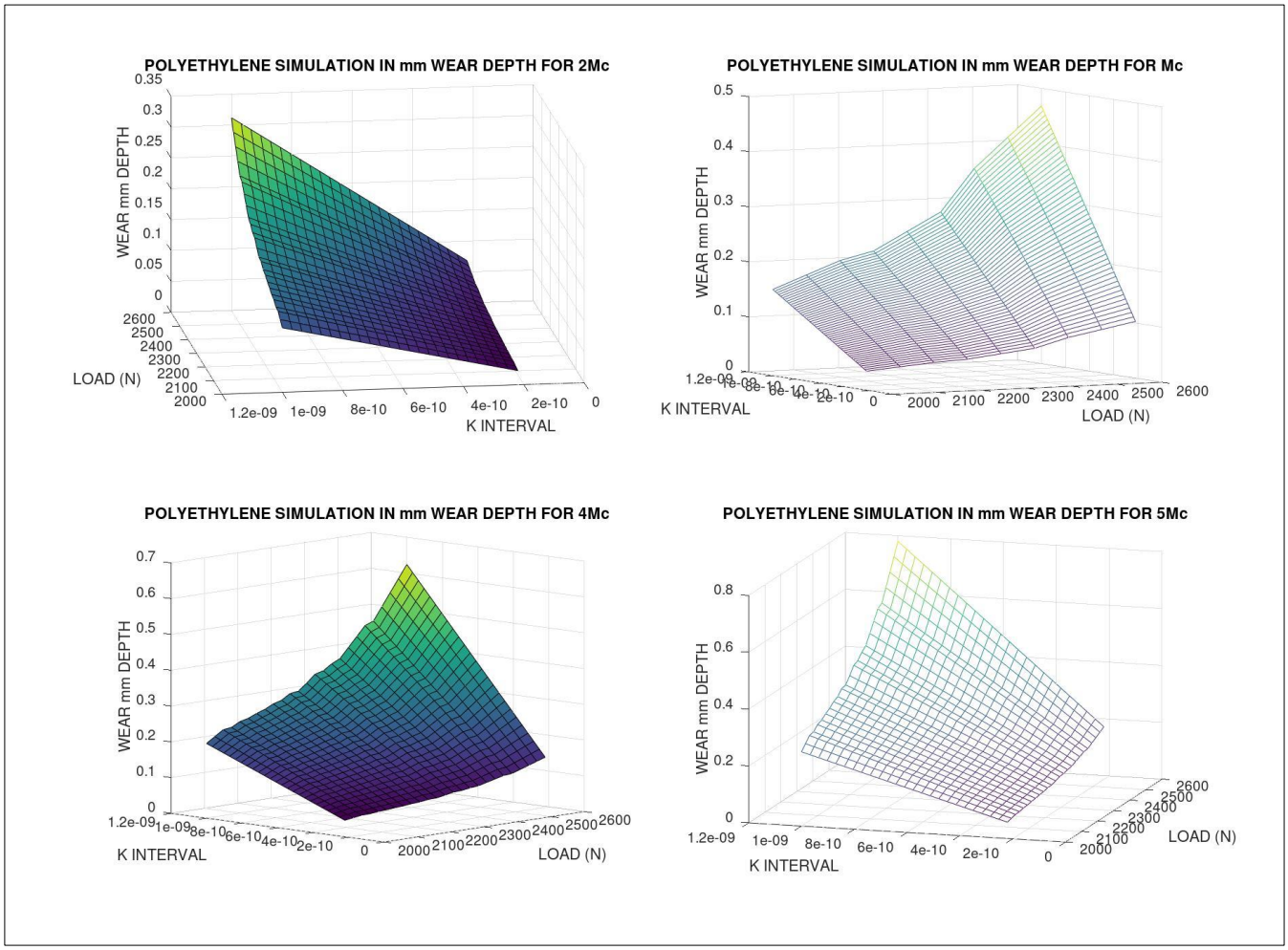

Figure 6.-Multiple simulation, 2 different 3D imaging processing subroutines, with GNU-Octave for (2-5) Mc. It is shown the basic model simulated in mm depth wear (when the surface contact is implemented, [1-8]). It shows the different wear magnitudes when Mc are increasing. The computational method, magnitude-parameters belong to Table 1. GNU-Octave imaging-processing is acceptable. This figure software is also developed in Matlab, Figure 2. [Casesnoves Bioengineering Laboratory Software 2025-k-3]. Note: at figures many times values axe-range of K_w are multiplied by 10^{-3} . This type of software is developed from Author's series of previous publications in hip prostheses wear and other computational contributions.

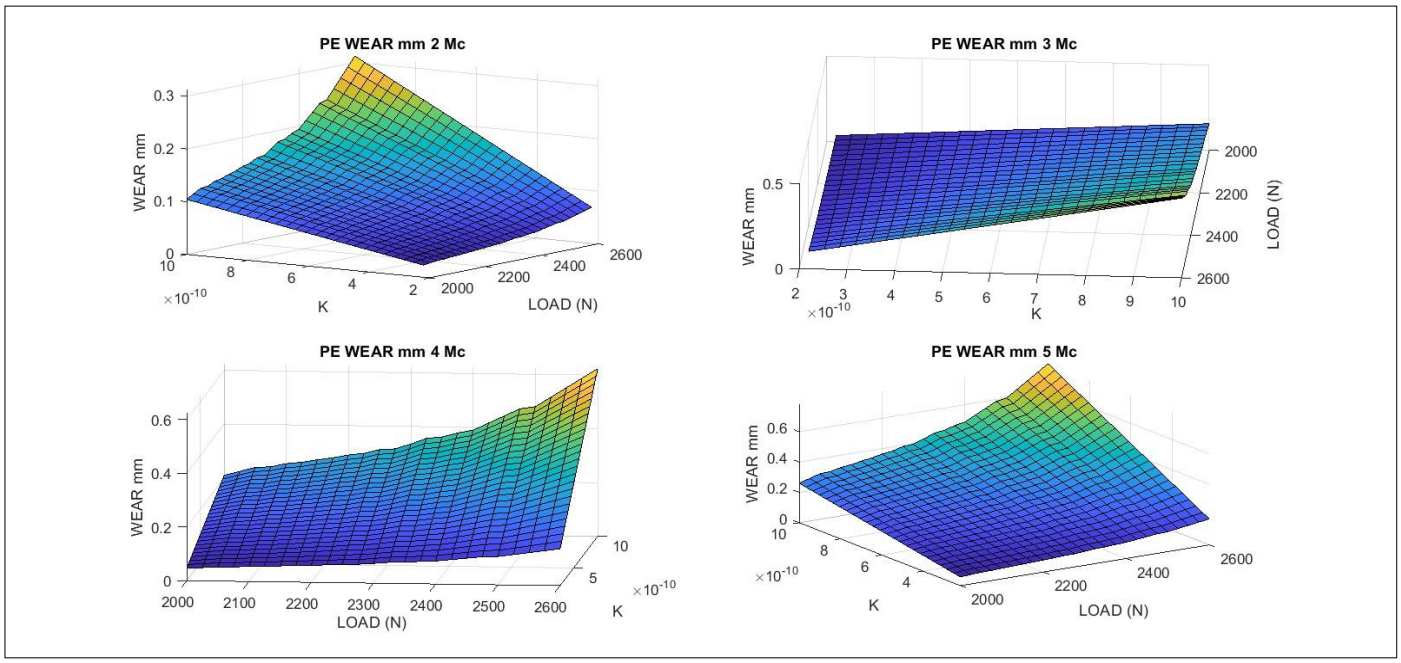

Figure 7.-Multiple simulation with Matlab, (2-5 Mc). It is shown the basic model simulated in wear mm Depth (when the surface area is implemented, [1-8]). It shows the different wear magnitudes when Mc are increasing. The computational method, magnitude-parameters belong to Tables 1-2. Note the K constant magnitude orders. Matlab image-processing is better than GNU-Octave in this case. [Casesnoves Bioengineering Laboratory Software 2025-k-4].

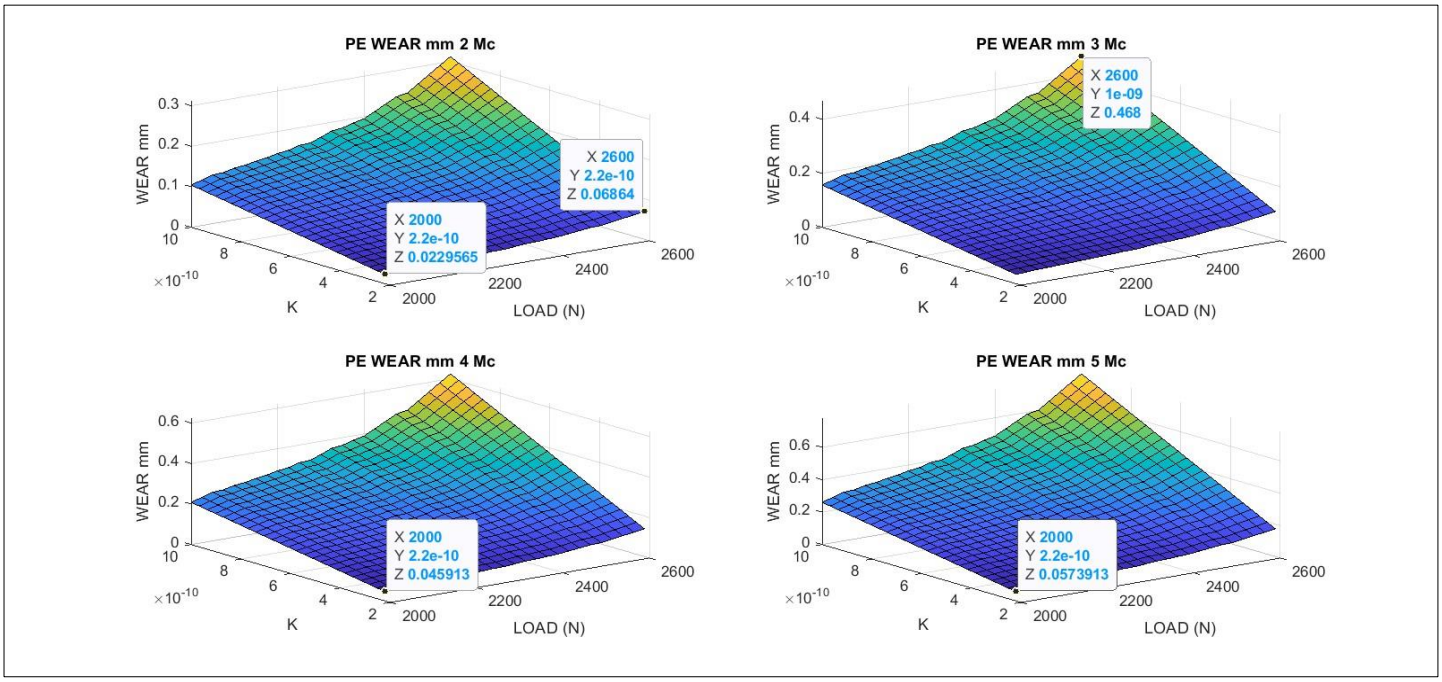

Figure 8.-From Figure 2, a number of dataset values implemented at image. That is, a number of graphical data for multiple simulation with Matlab, (2-5 Mc). It is shown the basic model simulated in wear mm Depth (when the surface area is implemented). It shows the different wear magnitudes when Mc are increasing. The computational method, magnitude-parameters belong to Table 1. Matlab image-processing is better than GNU-Octave in this case. [Casesnoves Bioengineering Laboratory Software 2025-k-5]

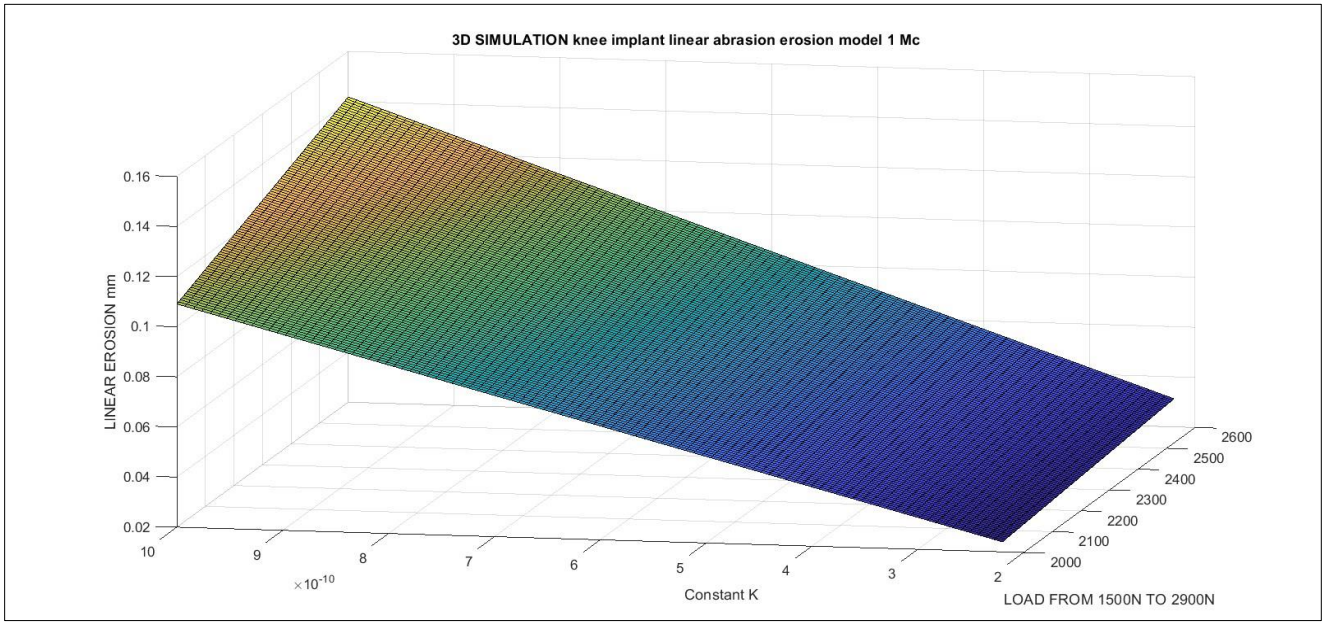

Figure 9.- Matlab graphical simulation with different simpler program for 1 Mc . It is shown the basic model simulated in wear mm Depth. It shows the different wear magnitudes when Loads are increasing. The computational method, magnitude-parameters belong to Tables 1-2. Matlab image-processing is better than GNU-Octave in this case. [Casesnoves Bioengineering Laboratory Software 2025-k-6] .

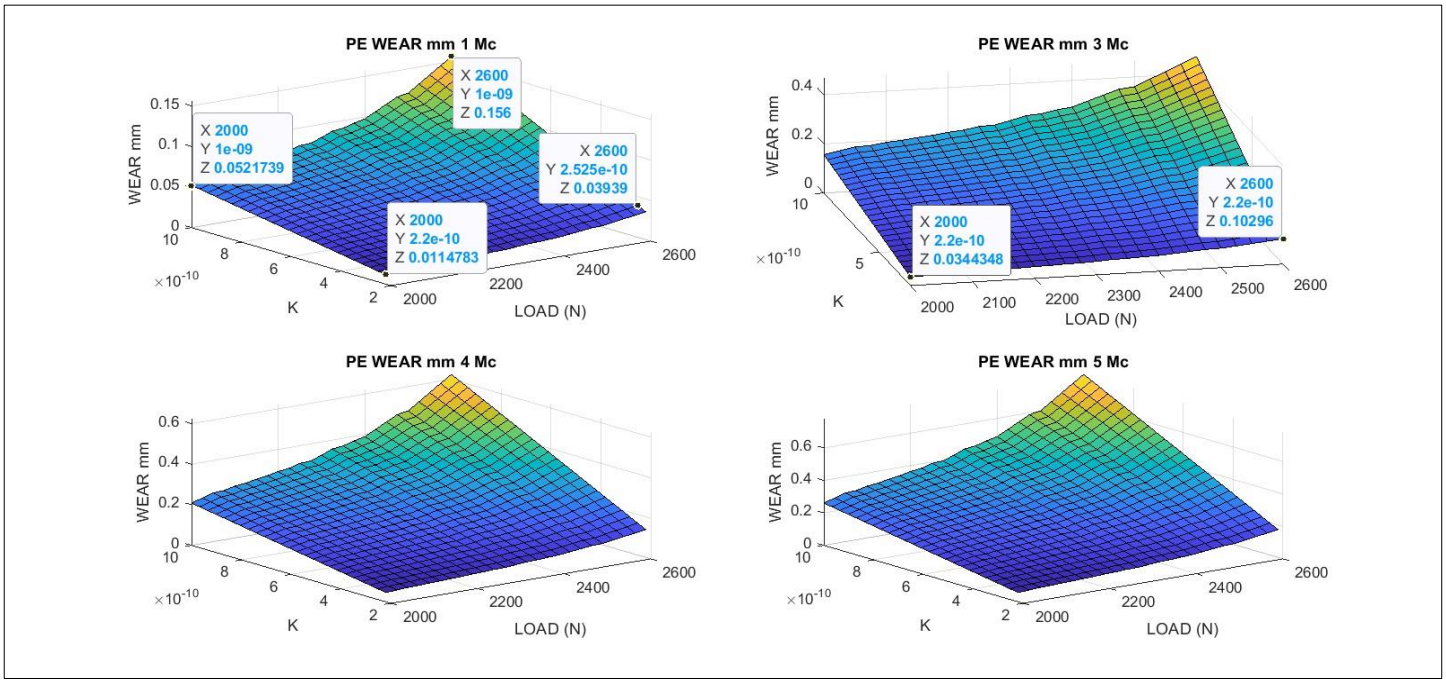

Figure 10.-For catching up the differences among 1 Mc and 3,4,5 Mc, it is shown a number of graphical data for multiple simulation with Matlab (dataset of 1 Mc included). Image-processing displays the different wear magnitudes when Mc are increasing. The computational method, magnitude-parameters belong to Table 1. Matlab image-processing is better than GNU-Octave in this case. [Casesnoves Bioengineering Laboratory Software 2025-k-7]

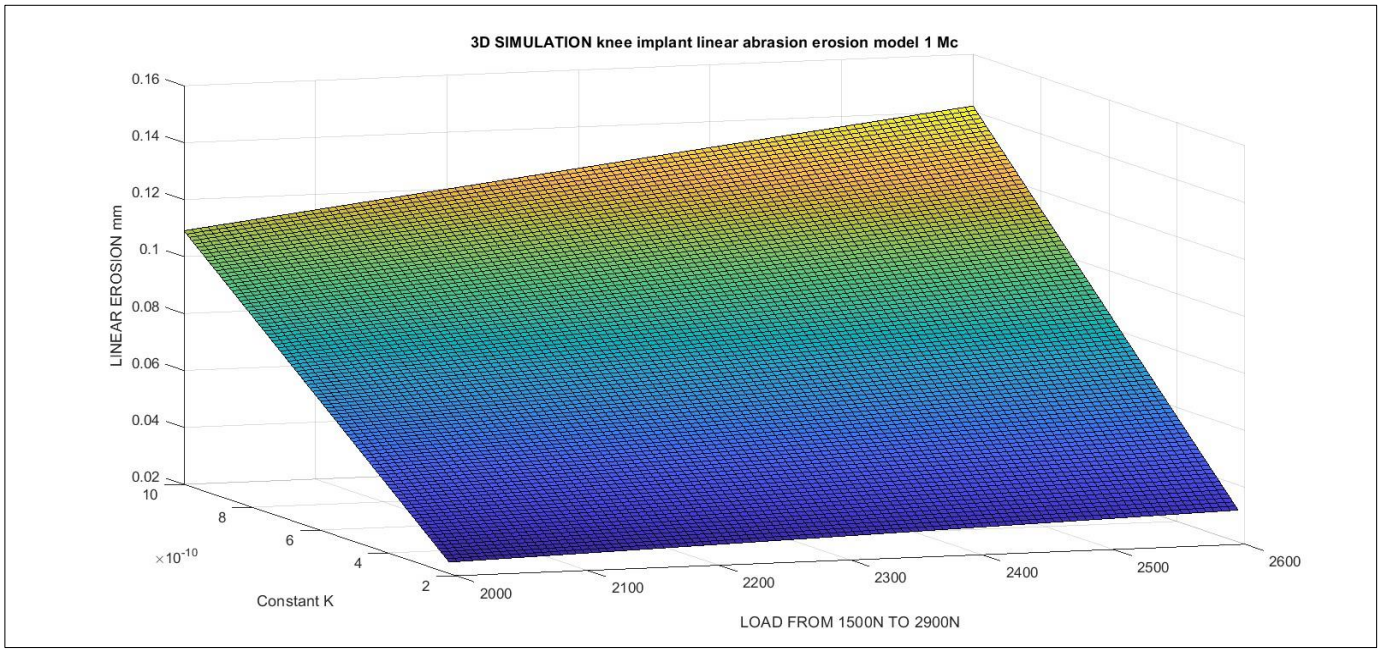

Figure 11.- A different perspective for software imaging-processing. Matlab graphical simulation with different simpler program for 1 Mc . It is shown the basic model simulated in wear mm Depth. It shows the different wear magnitudes when Loads are increasing. The computational method, magnitude-parameters belong to Tables 1-2. Matlab image-processing is better than GNU-Octave in this case. [Casesnoves Bioengineering Laboratory Software 2025-k-8]

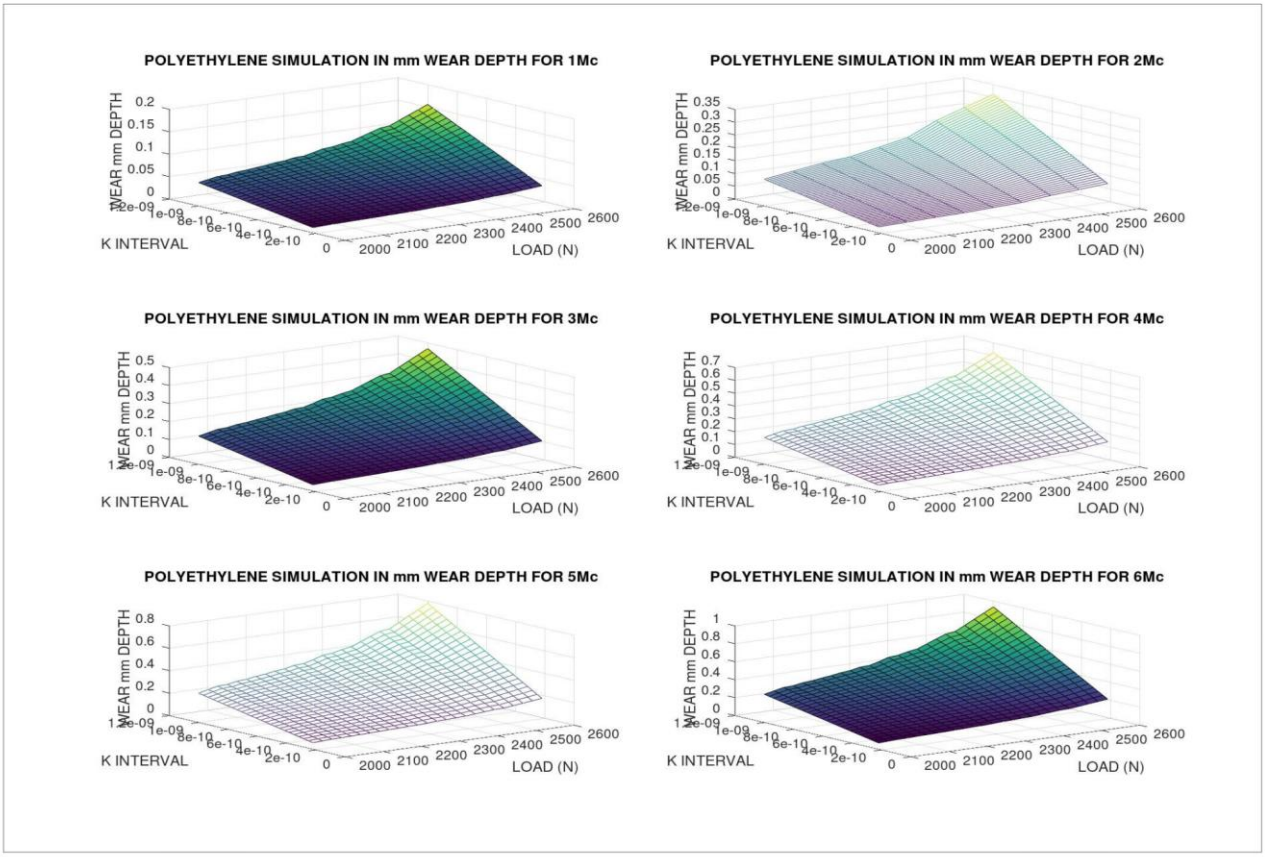

NUMERICAL RESULTS						
Mc	**RESULTS MINIMA**			**RESULTS MAXIMA**		
	WEAR (mm)	**K_w (mm^3 / (N x mm) x 10^{-3}**	**LOAD (N)**	**WEAR (mm)**	**K_w (mm^3 / (N x mm)**	**LOAD (N)**
1 Mc	0.01	2.2 x 10^{-10}	2000	0.16	10^{-9}	2600
2 Mc	0.02	2.2 x 10^{-10}	2000	0.31	10^{-9}	2600
3 Mc	0.03	2.2 x 10^{-10}	2000	0.46	10^{-9}	2600
4 Mc	0.05	2.2 x 10^{-10}	2000	0.62	10^{-9}	2600
5 Mc	0.06	2.2 x 10^{-10}	2000	0.78	10^{-9}	2600
COMMENTS	Almost linear the wear magnitudes. Intermediate values at Figures.			Less linear. Intermediate values at Figures.		

Figure 12.- Results 3D imaging processing composition for 1-6 Mc . GNU-Octave graphical simulation 1-6 Mc . Note the growing differences among maxima and minima from 1 Mc to 6 Mc. It is shown the basic model simulated in wear mm Depth. It shows the different wear magnitudes when Loads are increasing. The computational method, magnitude-parameters belong to Tables 1-2. Matlab image-processing is better than GNU-Octave in this case. [Casesnoves Bioengineering Laboratory Software 2025-k-9].

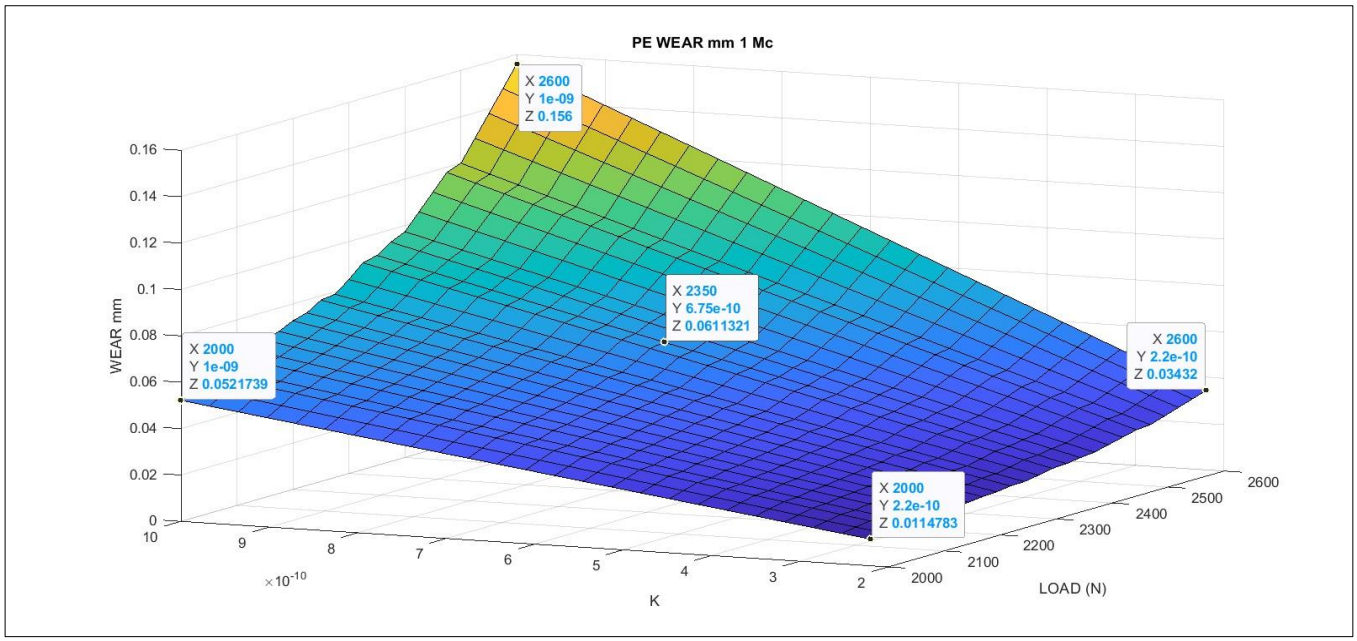

Figure 13.- Setting the display of dataset for Figures 9,11 . Matlab graphical simulation with different simpler program for 1 Mc . Note the differences among maxima and minima, and one random interior value. It is shown the basic model simulated in wear mm Depth. It shows the different wear magnitudes when Loads are increasing. The computational method, magnitude-parameters belong to Tables 1-2. Matlab image-processing is better than GNU-Octave in this case. [Casesnoves Bioengineering Laboratory Software 2025-k-10].

3.2 Numerical Results

Table 3 show extracted from Graphical Optimization the numerical data results for linear wear. At Table 4, Figures and magnitude orders are contrasted with standard literature [13-18]. For orthopedics wear implants and general software it is recommended to get ideas from [35, 36, 40, 41, 42, 43, 44, 45-51, 52, 53-63]. Figures 4-9 show all the Graphical Optimization results with dataset. The references [58-63] are intended for complementary further reading in polymer materials, biomechanics and tribology, recommended for the reader.

Table 3.- Main numerical results in the study. Magnitudes match standard literature, [13-18].

NUMERICAL RESULTS						
Mc	**RESULTS MINIMA**			**RESULTS MAXIMA**		
	WEAR (mm)	**K_W (mm^3 / (N x mm)) x 10^{-3}**	**LOAD (N)**	**WEAR (mm)**	**K_W (mm^3 / (N x mm)**	**LOAD (N)**
1 Mc	0.01	2.2×10^{-10}	2000	0.16	10^{-9}	2600
2 Mc	0.02	2.2×10^{-10}	2000	0.31	10^{-9}	2600
3 Mc	0.03	2.2×10^{-10}	2000	0.46	10^{-9}	2600
4 Mc	0.05	2.2×10^{-10}	2000	0.62	10^{-9}	2600
5 Mc	0.06	2.2×10^{-10}	2000	0.78	10^{-9}	2600
COMMENTS	Almost linear the wear magnitudes. Intermediate values at Figures.			Less linear. Intermediate values at Figures.		

3.3 Comparison of Numerical Results

Table 4 presents some numerical comparisons with other literature studies. Some of them are carried out with FE Method, others with FE Method and contrasted with cadaveric data. The most important objective consequence is that from [2,3] Mc on, the Linear Erosion shows a magnitude order jump from 10^{-2} to 10^{-1} mm. The comparisons are shown for database from [13-17]. However extensive further database can be found at [18-34].

Table 4.- Main numerical results in the study. The wear magnitudes and rates differ in literature and laboratories for two main reasons: (1) the large variety of testing apparatus and methods, and the ISO variants also, (2) the large variety to communicate/measure results. Namely, wear per Mc (mm), wear per year (mm), wear per Mc (mg), wear per year (mg), and others. When the study is in vivo, wear is usually expressed in mm/year, because the in vivo testing takes the sample data usually from patients or recent cadaveric samples whose medical histories show the date when the arthroplasty was done. What is common in all literature, is the polyethylene density approximately equal to water. Magnitude orders match standard literature, [3,11,13-18] . Additional complementary dataset can be found at [19-34]. FE method is used in general for both comparisons/validations with in vivo measurements. Computational Optimization and general Biotribology concepts can be read at [35-38].

COMPARATIVE NUMERICAL RESULTS

Mc [APPROX]	RESULTS APPROXIMATED FOR ALL COMPARISONS CALCULATIONS, WHEN IN VIVO, IT IS TAKEN FROM [16], AN AVERAGE OF 2Mc BY YEAR (STUDIES DIFFER ALSO)				
	AUTHOR'S STUDY LINEAR WEAR (mm)	1 [13, Hoshino and alt,wear+creep, 2002] [in vivo, 69 patients, geometrical extrapolation]	2 [14, Teeter, m, and alt, wear+creep, 2019] [in vivo, 49 patients] This author shows dataset for maximum wear, lateral (Lat), and medial (Med). It is shown [ref], Lat=[0.034,0.069]/year, and Med+[0.04,0.069]. All angles.	3 [15, Gascoyne and alt, wear+creep,2019] [in vivo, 106 patients] This Author shows 0.015 mm/year (supine), and 0.220 mm/year (standing). Proportional Average set by this study Author, is calculated here as, (4 x standing+supine) / 5 = 0.1790. Approx=0.18/year.	4 [17, Ozer, wear+creep,2022] [in vivo-in-vitro, FE compared to 1 cadaveric sample,Flex+AP, geometrical extrapolation]
1 Mc	[0.01,0.16]	[0.001,0.01]	LAT [0.02, 0.03] MED [0.02,0.03]	[0.09]	[0.03]
2 Mc	[0.02,0.31]	[0.01,0.20]	LAT [0.03,0.07] MED [0.04,0.07]	[0.18]	[0.08]
3 Mc	[0.03,0.46]	[0.50,1.00]	LAT [0.07,0.09] MED [0.06,0.09]	[0.27]	[0.09]
4 Mc	[0.05,0.62]	[1.00,1.10]	LAT [0.08,0.12] MED [0.08,0.12]	[0.36]	[0.10]
5 Mc	[0.06,0.78]	[1.10,1.20]	LAT [0.10,0.15] MED [0.10,0.15]	[0.45]	[0.13]
COMMENTS	Almost linear the wear magnitudes when Mc number is low, proportional to Mc number. Differences tend to get nonlinear in function of Mc, when the Mc magnitude increases.				
IMPORTANT DISCLAIMER	THE WEAR MAGNITUDES AND RATES DIFFER IN LITERATURE AND LABORATORIES FOR TWO MAIN REASONS: (1) THE LARGE VARIETY OF TESTING APPARATUS AND METHODS, (2) THE LARGE VARIETY TO COMMUNICATE/MEASURE RESULTS. NAMELY, WEAR PER Mc (mm), WEAR PER YEAR (mm), WEAR PER Mc (mg), WEAR PER YEAR (mg), AND OTHERS. WHEN THE STUDY IS IN VIVO, WEAR IS USUALLY EXPRESSED IN mm/YEAR. WHAT IS COMMON IS THE POLYETHYLENE DENSITY APPROXIMATELY EQUAL TO WATER.				

3.4 Biomaterials and Biomechanics TKA applications briefing

Table 5 shows a concise concept of study applications. The most important is the erosion rate prediction in order to find approximations for implant durability [37-58, 64-82]. Several other applications can be guessed from Table 5.

Table 5.- Biomechanical and Biotribological applications briefing. Some of them are similar to previous studies in hip joint wear [35,36].

APPLICATIONS BRIEFING	
PRINCIPAL UTILITY IN COMPUTATIONAL BIOENGINEERING	TKA Wear Predictions and efficacious calculations at 3D image-processing graphs, specially with Matlab, to know the exact magnitude for any selected K_W and Load (x, y, coordinates), the approximate abrasive wear magnitude for 1-5 Mc.
WEAR AND BIOTRIBOLOGY PREDICTIONS	For design/manufacturing of TKA prostheses. This is the most important utility. TKA erosion prediction, specially for polyethylene materials, is essential. Prediction saves manufacturing-research time, repeating laboratory work, and budget.
TKA DURABILITY PREDICTION	To provide patient with quality of life. To avoid re-operations and substitution for new prostheses.
INDUSTRIAL MANUFACTURING	Optimization of manufacturing process and improve quality.
I+D RESEARCH	The TKA prostheses are in continuous evolution. For future design of new types. Similar/variants of materials I+D.
PATIENT LIFE QUALITY	Very important for normal movement of patient. Walk and essential movements easy and comfortable for patient during all duration time.
SPORT MEDICINE	This is a very important application because sport-medicine requires these prostheses in higher quality than common patients.

4 CONCLUSIONS

The objectives of the research are to simulate the PE wear without creep models for TKA in a primary approximation. The models applied are initially for linear wear depth. Graphical Optimization for those models, numerical results, and comparison with literature dataset, Tables 1-2. Some recipes to develop simulation-software and a briefing application were included. At this stage, Lubrication Factors for the models were not set. Computational results and comparative results are included in Tables 3-4.

As a result, the computational model shows differences/advances, especially in the programming design, from previous publications. Because of the large variety of testing methods and laboratory apparatus, K_w published values vary in one magnitude order. One magnitude order for wear magnitude predictions is significative/important. Therefore, it comprises all published range of the linear wear

constant, K_w , namely [2.20 x 10^{-7} , 10^{-6}] implemented in arrays. Second, it plots in 2D-3D all the standard loads range, combined with the computational calculations (vectors) for Kw range. The literature research usually shows also a range of loads. For linear wear predictions, the Million Cycles range is set computationally at 2D-3D multiple-graphics in pattern combined with those loads and K_w ranges. The most significative finding is that from 2-3 Mc on, Linear wear (mm) increases from 10^{-2} magnitude order to 10^{-1} one.

5. Future Developments

The graphs obtained are acceptable and abrasive linear wear numerical results match approximately the standard dataset published. For 1 Mc abrasive linear wear is of the magnitude order around [10^{-2} , 10^{-1}]. The image processing quality in GNU-Octave and Matlab is acceptable. It was tried to approach the most common numerical and graphical results published, given the large amount of variants for mathematical models-methods and ISO for abrasive TKA implants predictions, Tables 3-4.

As commented in 2.1.1 Subsection, Friction coefficient was not implemented as it does not get any significant variation for results magnitude orders. However, for future studies will be set in numerical optimization refinements. Finite Elements method is widely set theoretically for simulations, and also compared with in vitro studies. In general, design/predictions of TKA implants is carried out with in vivo and/or in vitro data. In some cases the research is done with both methods, showing comparative or cadaveric results.

In brief, a Graphical Simulations-optimizations series for abrasive PE TKA implants were presented. Results match the literature figures and standards. Applications in Biotribology and Mathematical Optimization-Simulations are presented, Tables 3-4, Figure 7.

LIST OF ABBREVIATIONS

FE : Finite Elements method.

K_{wear} : Linear and Volume wear constant.

L_{wear} : Linear abrasive wear.

Mc : million cycles.

PE ; Polyethylene.

TKA: Total knee arthroplasty

UHMWPE : ultra high molecular weight polyethylene.

AUTHOR CONTRIBUTIONS

Author is sole responsible for conceptualization, computational-validation, dataset implemented, formal mathematical-programming analysis, visualization, investigation, methodology, formal-algorithms analysis, investigation, writing—original draft, writing—review.

AVAILABILITY OF DATA AND MATERIALS

The data underlying this study are available in the published article.

ETHICS COMMITTEE APPROVAL AND CONSENT TO PARTICIPATE

This study does not include experiments, testing, laboratory, apparatus, that require approval from an ethics committee. All experiments were conducted with computational intelligence based on open access literature. Then, does not necessitate such permissions.

CONSENT FOR PUBLICATION

Not applicable.

CONFLICTS OF INTEREST

The authors declare no conflicts of interest regarding this manuscript.

FUNDING

Independent funding from prospective Independent Bioengineering Laboratory (doing/preparing registration as company), no funding number was provided.

ACKNOWLEDGMENTS

The author gratefully acknowledges the reviewers for their valuable comments and for helping improve the clarity and formal grammar of the manuscript.

All figures and Sketchs are done with Author's Software and GNU-Octave and Matlab systems. The unique Figure (modified by Author) is Figure 1. [Google free images, Dr Albrecht, knee and cartilague specialist], modified and drawn by Francisco Casesnoves. The software and algorithms are original from the Author, (namely, the integral linear wear model), or based on recognized publications. The Systems used, Matlab and GNU-Octave, are formally recognized.

The authors confirm that all content of the manuscript (including figures), was developed without the use of artificial intelligence or AI-assisted technologies.

REFERENCES

[1] Dawim, P; (2013). *Biomaterials and medical tribology . Research and development*. Woodhead Publishing. 2013.

[2] Schaldach, M ; Hohmann, D; (1976). *Advances in artificial hip and knee joint technology*. Springer. 1976.

[3] Jin, Z; (2014). *Computational Modelling of Biomechanics and Biotribology in the Musculoskeletal System*. Woodhead Publishing .2014.

[4] Munzinger, U; Boldt, J; Keblish, P; (2004). *Primary knee arthroplasty*. Springer 2004.

[5] Dawim, P.J. (2010). *Biotribology*. Wiley. 2010, ISBN: 978-1-848-21275-6.

[6] Sculco, T; Martucci, E; (2001). Knee Arthroplasty. Springer. 2001.

[7] Emre Tokgoz, E; and Colls; (2023). T*otal Knee Arthroplasty A Review of Medical and Biomedical Engineering and Science Concepts*. Springer. 2023.

[8] Kumar, A; and Colls; (2024). *Applications of Biotribology in Biomedical Systems*. Springer. 2024.

[9] Kretzer, J; (2014) . Wear in total knee arthroplasty—just a question of polyethylene? . International Orthopaedics (SICOT) (2014) 38:335–340 . DOI 10.1007/s00264-013-2162-4 . 2014.

[10] D'Lima, D; (2007). Doctoral Thesis. *In vivo tibial force measurement after total knee arthroplasty*. UC San Diego Electronic Theses and Dissertations. 2007.

[11] Affatato, S; (2012). *Wear of orthopaedic implants and artificial joints*. Woodhead Publishing Limited. 2012.

[12] Triwardono, J; and Colls; (2021). *Evaluation of the Contact Area in Total Knee Arthroplasty Designed for Deep Knee Flexion*. International Journal of Technology 12(6) 1312-1322 (2021) . DOI: 10.14716/ijtech.v12i6.5193 . http://ijtech.eng.ui.ac.id .

[13] Hoshino, A; and Colls; (2002). *Accurate in vivo measurement of polyethylene wear in Total Knee Arthroplasty*. The journal of Arthroplasty. Vol 17, No. 4. 2002.

[14] Teeter, M; and Colls; (2019). *Radiostereometric analysis permits in vivo measurement of very small levels of wear in TKA*. Clin Orthop Relat Res (2019) 477:80-90. DOI 10.1097/CORR.0000000000000399.

[15] Gascoyne, T; and Colls; (2019). *In vivo wear measurement in a modern total knee arthroplasty with model-based radiostereometric analysis*. Bone & Joint Journal 2019;101-B:1348–1355.

[16] Silva, M; and Colls; (2002). *Average patient walking activity approaches 2 million cycles per year. pedometers under-record walking activity*. The journal of Arthroplasty. Vol 17, No. 6. 2002.

[17] Ozer, A; (2022). *Computational wear of knee implant polyethylene insert surface under continuous dynamic loading and posterior tibial slope variation based on cadaver experiments with comparative verification*. BMC Musculoskeletal Disorders, (2022) 23:871. https://doi.org/10.1186/s12891-022-05828-2 .

[18] Heisel, C; and Colls; (2004). *Short-term in vivo wear of cross-linked polyethylene*. The Journal of Bone and Joint Surgery · April 2004. DOI: 10.2106/00004623-200404000-00012 . PubMed.

[19] Abdelgaied, A; and Colls; (2011). *Computational wear prediction of artificial knee joints based on a new wear law and formulation*. Journal of Biomechanics 44 (2011) 1108–1116 . Elsevier. 2011.

[20] Pecora, J; Romero, V; (2020). *Evaluation of Polyethylene Wear in a Brazilian Ultracongruent Knee Prosthesis with a Rotating Platform*. Rev Bras Ortop 2021;56(1):42–46. 2021.

[21] Soni, A; (2020). *Total Knee Arthroplasty (TKA) Wear Analysis on the Tibial Implant using Finite Element Method Approach*. International Journal of All Research Education and Scientific Methods (IJARESM) ISSN: 2455-6211, Volume 6, Issue 1, January- 2018, Impact Factor: 2.287. 2020.

[22] Bergmann, G; and Colls (2014). *Standardized Loads Acting in Knee Implants*. PLOS one . January 2014 | Volume 9 | Issue 1 | e86035 .

[23] Dreyer, M; and Colls; (2022). *European Society of Biomechanics S.M. Perren Award 2022: Standardized tibio-femoral implant loads and kinematics* . Journal of Biomechanics 141 (2022) 111171. Elsevier.

[24] Innocenti, B; and Colls; (2014). *Development and Validation of a Wear Model to Predict Polyethylene Wear in a Total Knee Arthroplasty: A Finite Element Analysis*. Lubricants 2014, 2, 193-205; doi:10.3390/lubricants2040193 . 2014.

[25] De Ruiter, L; and Colls; (2020) . *The Effects of Cyclic Loading and Motion on the Implant–Cement Interface and Cement Mantle of PEEK and Cobalt–Chromium Femoral Total Knee Arthroplasty Implants: A Preliminary Study* . MDPI. Materials 2020, 13, 3323; doi:10.3390/ma13153323 . 2020.

[26] Kumar, V; and Colls; (2023). *Triboinformatic Modeling of Wear in Total Knee Replacement Implants Using Machine Learning Algorithms*. Journal of Materials and Engineering Vol. 01, Iss. 3 (2023) 97-105 . 2023.

[27] Fisher, J; and Colls; (2001). *Wear of polyethylene in artificial knee joints*. Current Orthopaedics (2001) 15, 399d405 . Elsevier. 2001.

[28] Fuchs, S; and Colls (2000). *Retropatellar contact characteristics in total knee arthroplasty with and without patellar resurfacing*. International Orthopaedics (SICOT) (2000) 24:191–193. Springer.2000.

[29] Koh, Y; et al. ; (2020). *Prediction of wear performance in femoral and tibial conformity in patient-specific cruciate-retaining total knee arthroplasty* . Journal of Orthopaedic Surgery and Research (2020) 15:24. Journal of Orthopaedic Surgery and Research https://doi.org/10.1186/s13018-020-1548-4 . 2020.

[30] Stukenborg-Colsman, C; et al. ; (2002). *Tibiofemoral contact stress after total knee arthroplasty*. Acta Orthop Scand 2002; 73 (6):638-646 . 2002.

[31] Uvehammer, J; (2001). Doctoral Thesis. *Knee joint kinematics, fixation and function related to joint area design in total knee arthroplasty*. Acta Orthopaedica Scandinavica Supplementum no. 299, vol. 72. 2001.

[32] A. Abdelgaied, A; Fisher, J; Jennings, L; (2022). *Understanding the differences in wear testing method standards for total knee replacement*. Journal of the Mechanical Behavior of Biomedical Materials 132 (2022) 105258 . Elsevier. 2022.

[33] Dai, Y; et al. ; (2014). *Increased shape and size offerings of femoral components improve fit during total knee arthroplasty*. Knee Surg Sports Traumatol Arthrosc (2014) 22:2931–2940.DOI 10.1007/s00167-014-3163-6 . 2014.

[34] Fekete, G: et al.; (2017). *Tibiofemoral wear in standard and non-standard squat: implication for total knee arthroplasty*. Muscles, Ligaments and Tendons Journal 2017;7 (4):520-528 . 2017.

[35] Casesnoves, F. *Multiobjective Optimization for Ceramic Hip Arthroplasty with Medical Physics Applications*. Int. J. Sci. Res. Comput. Sci. Eng. Inf. Technol. 2021, 7, 582–598. [CrossRef]

[36] Casesnoves, F. *Nonlinear comparative optimization for biomaterials wear in artificial implants technology*. In Proceedings of the Applied Chemistry and Materials Science RTU2018 Conference Proceedings, Riga, Latvia, 26 October 2018.

[37] Merola, M.; Affatato, S. *Materials for Hip Prostheses: A Review of Wear and Loading Considerations*. Materials 2019, 12,495. [CrossRef] .

[38] Navarro, N. *Biomaterials in orthopaedics*. J. R. Soc. Interface 2008, 5, 1137–1158. [CrossRef] .

[39] Sachin, G.; Mankar, A.; Bhalerao, Y. *Biomaterials in Hip Joint Replacement*. Int. J. Mater. Sci. Eng. 2016, 4, 113–125. [CrossRef]

[40] Casesnoves, F. *2D computational-numerical hardness comparison between Fe-based hardfaces with WC-Co reinforcements for Integral-Differential modelling*. Trans. Tech. 2018, 762, 330–338. [CrossRef] .

[41] Casesnoves, F.; Antonov, M.; Kulu, P. *Mathematical models for erosion and corrosion in power plants. A review of applicable modelling optimization techniques*. In Proceedings of RUTCON2016 Power Engineering Conference, Riga, Latvia, 13 October 2016.

[42] Casesnoves, F. *Die Numerische Reuleaux-Methode Rechnerische und Dynamische Grundlagen mit Anwendungen (Erster Teil).* Sciencia Scripts, 2019; ISBN-13 978-620-0-89560-8.

[43] Kulu, P.; Casesnoves, F.; Simson, T.; Tarbe, R. *Prediction of abrasive impact wear of composite hardfacings. Solid State Phenomena*. In Proceedings of the 26th International Baltic Conference on Materials Engineering, Vilnius, Lithuania, 26–27 October 2017; Trans Tech Publications: Bäch, Switzerland, 2017; Volume 267, pp. 201–206. [CrossRef] .

[44] Casesnoves, F. *Mathematical Models and Optimization of Erosion and Corrosion*. Ph.D. Thesis, Taltech University, Evaluated as excellent, Tallinn, Estonia, 14 December 2018.

[45] Casesnoves, F. *The Numerical Reuleaux Method, a Computational and Dynamical Base with Applications. First Part.* Lambert Academic Publishing: Republic of Moldava, 2019; ISBN-10 3659917478.

[46] Casesnoves, F. *Large-Scale Matlab Optimization Toolbox (MOT) Computing Methods in Radiotherapy Inverse Treatment Planning*. High Performance Computing Meeting; Nottingham University: Nottingham, UK, 2007.

[47] Casesnoves, F. *A Monte-Carlo Optimization method for the movement analysis of pseudo-rigid bodies*. In Proceedings of the 10th SIAM Conference in Geometric Design and Computing, San Antonio, TX, USA, 4–8 November 2007. Contributed Talk.

[48] Casesnoves, F. *Theory and Primary Computational Simulations of the Numerical Reuleaux Method (NRM)*. Int. J. Math. Computation 2011, 13, 89–111. Available online: http://www.ceser.in/ceserp/index.php/ijmc/issue/view/119 (accessed on 28 June 2021).

[49] Casesnoves, F. *Applied Inverse Methods for Optimal Geometrical-Mechanical Deformation of Lumbar artificial Disks/Implants with Numerical Reuleaux Method. 2D Comparative Simulations and Formulation*. Comput. Sci. Appl. 2015, 2, 1–10. Available online: www.ethanpublishing.com (accessed on 28 June 2021).Standards 2021, 1 .

[50] Casesnoves, F. *Inverse methods and Integral-Differential model demonstration for optimal mechanical operation of power plants–numerical graphical optimization for second generation of tribology models*. Electr. Control Commun. Eng. 2018, 14, 39–50. [CrossRef] .

[51] Casesnoves, F.; Surzhenkov, A. I*nverse methods for computational simulations and optimization of erosion models in power plants*. In Proceedings of the IEEE Proceedings of RUTCON2017 Power Engineering Conference, Riga, Latvia, 5 December 2017. [CrossRef] .

[52] Casesnoves, F. *Exact Integral Equation Determination with 3D Wedge Filter Convolution Factor Solution in Radiotherapy*. Series of Computational-Programming 2D-3D Dosimetry Simulations. Int. J. Sci. Res. Sci. Eng. Technol. 2016, 2, 699–715.

[53] Casesnoves, F. *Software Programming with Lumbar Spine Cadaveric Specimens for Computational Biomedical Applications*. Int. J. Sci. Res. Comput. Sci. Eng. Inf. Technol. 2021, 7, 7–13.

[54] Surzhenkov, A.; Viljus, M.; Simson, T.; Tarbe, R.; Saarna, M.; Casesnoves, F. *Wear resistance and mechanisms of composite hardfacings atabrasive impact erosion wear*. J. Phys. 2017, 843, 012060. [CrossRef] .

[55] Casesnoves, F. *Computational Simulations of Vertebral Body for Optimal Instrumentation Design. ASME J. Med*. Devices 2012, 6, 021014. [CrossRef] .

[56] Barker, P. *The effect of applying tension to the lumbar fasciae on segmental flexion and extension*. In Proceedings of the 5th International Congress of Low Back and Pelvic Pain, Melbourne, Australia, 10–13 November 2014; pp. 50–52.

[57] European Textbook on Ethics in Research. European Commission, Directorate-General for Research. Unit L3. Governance and Ethics. European Research Area. Science and Society. EUR 24452 EN. Available online: https://op.europa.eu/en/publication-detail/-/publication/12567a07-6beb-4998-95cd-8bca103fcf43 (accessed on 28 June 2021).

[58] ALLEA. *The European Code of Conduct for Research Integrity, Revised ed*. ALLEA: Berlin, Germany, 2017.

[59] Bains, P; et al. *Biomaterials in Orthopaedics and Bone Regeneration*. Springer. 2019.

[60] Stergiou, N. *Biomechanics and Gait Analysis. Academic Press*. 2020.

[61] Tanzi, M;Fare, S. *Characterization of Polymeric Biomaterials.* Woodhead Publishing Series in Biomaterials . 2021.

[62] Okuno, E; Fratin, L. *Biomechanics of the Human Body*. Springer. 2014.

[63] Abhilash, P; et al. *Bioimplants Manufacturing . CRC Press. 2025.*

[64]. Kurtz, S. *Advances in Zirconia Toughened Alumina Biomaterials for Total Joint Replacement*. J. Mech. Behav. Biomed. Mater. 2014, 31, 107–116. [CrossRef]

[65] Li, Y.; Yang, C.; Zhao, H.; Qu, S.; Li, X.; Li, Y. *New Developments of Ti-Based Alloys for Biomedical Applications*. Materials 2014, 7, 1709–1800. [CrossRef]

[66] Kolli, R.; Devaraj, A. *A Review of Metastable Beta Titanium Alloys*. Metals 2018, 8, 506. [CrossRef] .

[67] Holzwarth, U.; Cotogno, G. *Total Hip Arthroplasty*. JRC Scientific and Policy Reports; European Commission: Brussels, Belgium, 2012.

[68] Delimar, D. *Femoral head wear and metallosis caused by damaged titanium porous coating after primary metal-on-polyethylene total hip arthroplasty: A case report*. Croat. Med. J. 2018, 59, 253–257. [CrossRef] [PubMed]

[69] Zhang, M.; Fan, Y. *Computational Biomechanics of the Musculoskeletal System.* CRC Press: Boca Raton, FL, USA, 2015.

[70] Dreinhöfer, K.; Dieppe, P.; Günther, K.; Puhl, W. Eurohip. *Health Technology Assessment of Hip Arthroplasty in Europe.* Springer: Berlin/Heidelberg, Germany, 2009.

[71] Hutchings, I.; Shipway, P. *Tribology Friction and Wear of Engineering Materials, 2nd ed*. Elsevier: Amsterdam, The Netherlands, 2017.

[72] Shen, X.; Lei, C.; Li, R. *Numerical Simulation of Sliding Wear Based on Archard Model*. In Proceedings of the 2010 International Conference on Mechanic Automation and Control Engineering, Wuhan, China, 26–28 June 2010. [CrossRef] .

[73] Affatato, S.; Brando, D. *Introduction to Wear Phenomena of Orthopaedic Implants.* Woodhead Publishing: Sawston, UK, 2012.

[74] Matsoukas, G.; Kim, Y. *Design Optimization of a Total Hip Prosthesis for Wear Reduction*. J. Biomech. Eng. 2009, 131, 051003. [CrossRef] [PubMed] .

[75] Galante, J.; Rostoker, W. *Wear in Total Hip Prostheses*. Acta Orthop. Scand. 2014, 43, 1–46. [CrossRef] [PubMed] .

[76] Mattei, L.; DiPuccio, F.; Piccigallo, B.; Ciulli, E. *Lubrication and wear modelling of artificial hip joints: A review*. Tribol. Int. 2011, 44, 532–549. [CrossRef] .

[77] Jennings, L. *Enhancing the safety and reliability of joint replacement implants*. Orthop. Trauma 2012, 26, 246–252. [CrossRef] [PubMed] .

[78] Saifuddin, A.; Blease, S.; Macsweeney, E. *Axial loaded MRI of the lumbar spine*. Clin. Radiol. 2003, 58, 661–671. [CrossRef] .

[79] Damm, P. *Loading of Total Hip Joint Replacements*. Ph.D. Thesis, Technischen Universität, Berlin, Germany, 2014.

[80] Abramobitz, S. *Handbook of Mathematical Functions*. Appl. Math. Ser. 1972, 55.

[81] Luenberger, G.D. *Linear and Nonlinear Programming, 4th ed.* Springer: Berlin/Heidelberg, Germany, 2008.

[82] Panjabi, M.; White, A. *Clinical Biomechanics of the Spine*. Lippincott 1980, 42, S3.